 https://doi.org/10.3311/PPme.38242

Periodica Polytechnica Mechanical Engineering, 68(4), pp. 336–345, 2024

Quantifying the Tip Leakage Vortex Wandering in a Low-Speed Axial Flow Fan via URANS Simulation

Bálint Lendvai[1*], Tamás Benedek[1]

[1] Department of Fluid Mechanics, Faculty of Mechanical Engineering, Budapest University of Technology and Economics, H-1111 Budapest, Műegyetem rkp. 3., Hungary
[*] Corresponding author, e-mail: lendvai.balint@gpk.bme.hu

Received: 02 September 2024, Accepted: 18 October 2024, Published online: 05 November 2024

Abstract

The tip leakage vortex is a dominant noise and aerodynamic loss source of low-speed axial flow fans. The tip leakage vortex often has an unsteady behavior, like the periodic motion of the vortex core: the so-called vortex wandering. This periodic vortex wandering results in additional noise, aerodynamic loss, and an oscillation in the moment acting on the blading, which causes an unfavorable vibration of the rotor. In the research campaigns focusing on vortex wandering, complicated measurement techniques (PIV) or high-fidelity but computationally costly simulations are commonly used. The present paper aims to introduce a relatively cost-effective unsteady Reynolds-averaged Navier-Stokes simulation-based investigation method of vortex wandering. The capabilities of the proposed technique are presented through a low-speed axial flow fan case study.

Keywords

low-speed fan, tip leakage vortex, vortex wandering, CFD, URANS

1 Introduction

Low-speed axial flow fans are widespread both in industrial applications and in households as well. Therefore, high-efficiency and low noise-emission fans are in high demand. Still, one of the significant sources of both losses and sound emission is the inevitable tip leakage flow, which can cause up to nearly a third of the hydraulic losses of the fan and, in many cases, has been identified as the dominant sound source [1–3]. In the case of axial flow fans, tip leakage flow rolls up and forms the tip leakage vortex (TLV). It has been suggested that after rollup, the TLV core starts spiraling as it propagates downstream in the blade passage [2, 4] while following the curvature of the casing in the case of ducted turbomachines.

Fukano and Jang [2] conducted corotating hot-wire probe measurements on a low-speed axial flow fan at design and off-design operating conditions. Cross-correlation of the velocity data indicated a spiral-type vortical structure, which causes a low-frequency tonal noise as it interacts with the blade and casing surface. Also, the peak frequency of the velocity fluctuation is directly proportional to the rotational speed of the rotor. Tan et al. [4] investigated a one and a half stage compressor with a transparent casing. Based on the cavitating vortex trace, high-speed imaging revealed the spiraling trajectory of the TLV core. Aeroacoustic simulations were carried out by Zhu et al. [5] using the Lattice-Boltzmann method. Low-frequency, rotating coherent flow structures were detected in the tip region of the rotor blade.

The unsteady behavior of the spiraling tip leakage vortex is well-documented in the case of axial flow turbomachines [6]. This seemingly arbitrary motion of the vortex core around its temporarily averaged location is called vortex wandering. The vortex wandering phenomenon of the TLV in the case of axial flow fans has been shown with particle image velocimetry (PIV) measurement [7, 8] and has been reproduced with simulation [9, 10] as well.

Jin et al. [7] experienced the natural unsteady behavior of the TLV of both forward and backward-skewed low-speed fans in PIV measurements for off-design operating conditions. The vortex cores were identified by local relative velocity minimum and vorticity maximum. The detected instantaneous cores were randomly scattered approximately in an ellipse. The most significant deviation of the TLV core was 6.4% of the tip chord length in the azimuthal direction.

Lee et al. [8] investigated the TLV wandering in a forward-swept low-speed fan of an AC outdoor unit with PIV measurements. The measurements were carried out at

Cite this article as: Lendvai, B., Benedek, T. "Quantifying the Tip Leakage Vortex Wandering in a Low-Speed Axial Flow Fan via URANS Simulation", Periodica Polytechnica Mechanical Engineering, 68(4), pp. 336–345, 2024. https://doi.org/10.3311/PPme.38242

stall, peak efficiency, and two higher flow rate operating conditions. Similarly, the instantaneous vortex core pattern showed an ellipse-like distribution with the largest displacement in the circumferential direction. Also, it was found that the magnitude of the vortex motion increases as the TLV travels downstream in the blade passage.

Boudet et al. [9] performed zonal large eddy simulations on an axial flow fan focusing on the tip leakage flow. Natural unsteadiness was observed in the simulation based on coincident acoustic spectrum and velocity fluctuation. Also, the Fourier transform of the field variables indicate tip leakage flow oscillation at the frequency of the natural unsteadiness. Thus, it was concluded that the TLV wandering was caused by either upstream casing-induced turbulence instabilities or rotating instability.

A high-resolution large eddy simulation of an AC outdoor unit fan at design condition was carried out by Park et al. [10]. The TLV was found to be oscillating around the temporarily averaged vortex core location at a low frequency. The frequency of the oscillation could be identified based on the local axial velocity time series. The motion of the TLV was mainly in the azimuthal direction. Locally increased turbulent kinetic energy, which promotes losses around the vortex core, was reported by both Park et al. [10] and Lee et al. [8], which was due to the natural unsteadiness.

The frequency of the vortex wandering can also be expressed with the nondimensional frequency called the Strouhal number. However, the method of nondimensionalizing the frequency is ambiguous as numerous velocity scales (blade tip velocity, inflow relative velocity) and length scales (chord length, tip clearance size, radius, solidity) or their combination may influence the phenomenon. Park et al. [10] calculated the Strouhal number to be 1.0 based on blade tip radius and velocity. This is supported by the findings of Fukano and Jang [2], as they reported that the frequency of the velocity fluctuation is directly proportional to the fan rotational speed. However, this Strouhal number definition is unfavorable as it suggests that the vortex wandering frequency is independent of the operating point of the turbomachine, while it is known that the TLV development is highly affected by the operating condition. Also, Fukano and Jang [2] found that decreasing the flow rate at constant rotational speed decreases the velocity fluctuation frequency. It was also reported that increased tip clearance size significantly reduced the characteristic frequency of the velocity fluctuation.

On the other hand, Boudet et al. [9] computed the Strouhal number of the vortex wandering to be 1.0 based on relative streamwise velocity at the blade tip and blade tip chord length. Using identical variables, You et al. [11] calculated the vortex wandering Strouhal number to be 1.5. This definition is more suitable as the local velocity and geometric features directly influence the tip leakage vortex phenomenon. Clearly, the Strouhal number definitions listed above are not equivalent, and the identical numerical value is merely a coincidence. Also, Jin et al. [7] reported natural unsteadiness over a wider frequency range, thus, a unique Strouhal number is not straightforward.

The investigation of the unsteady nature of the TLV is further obstructed as the vortex core detection and flow visualization are challenging in the case of turbomachinery. In both measurement and numerical simulation results, the tip vortex is mainly represented by streamlines or a simple vortex region identification method such as the λ_2 [12] and the Q criterion [13]. However, these commonly used flow visualization techniques are for vortex region detection, and they are not able to determine the location of the core, i.e., the position of the vortex. Thus, these methods are sufficient for qualitative findings, but quantitative results cannot be filtered out. In contrast to vortex region detection and flow visualization methods, vortex core detection techniques are able to track the motion of the vortex core; thus, the change in the vortex location over time can also be quantified [14].

The most straightforward vortex core line detection technique would be to look for local line type extrema of quantities associated with vortex cores, such as pressure minima, vorticity maxima, and helicity density maxima [15]. Thus, ridge line detection methods could be implemented for vortex core detection, such as the pseudo-pressure valley detection of Miura and Kida [16]. However, these ridge detection algorithms require higher order derivatives of said quantities, which are computationally costly to calculate, and extremely fine mesh resolution is necessary for increased accuracy. Also, it is suggested that these quantities in themselves are incapable of describing the vortex skeleton since both pressure and vorticity are drastically affected by the flow features [14]. For instance, solid surfaces submerged in fluid flows produce high vorticity and pressure deviations comparable to, if not stronger than, the vortex itself.

A different approach was presented by Jiang et al. [17]. It was suggested to look for locations where the velocity field of the neighboring cells describes a closed loop in a plane. This step narrows down the potential locations of the vortices, and then a computationally more costly local

vortex identification method is carried out at the previously marked locations. The technique is easily applicable for 2D cases; however, in the case of 3D simulations, choosing the plane perpendicular to the vortex core in which the velocity field shall be evaluated is not straightforward.

Another vortex core line method was presented by Sujudi and Haimes [18]. First, only regions having complex eigenvalue velocity Jacobians were considered, and the vortex core was defined where the velocity is parallel with the real eigenvector of the velocity Jacobian. Assuming steady state flow, this can be further interpreted as the locations where the velocity field is parallel with the acceleration field. This is equivalent to streamlines with zero curvature, meaning a particle moving on a locally straight line. However, in the case of strongly curved vortices, a higher-order vortex identification method is required, such as the method proposed by Roth and Peikert [19] for detecting the vortex line. The technique assumes bent vortices with zero-torsion. With this presumption, the vortex core line is defined as the set of points where the local velocity is parallel to its second total derivative. This method can successfully localize heavily curved vortex cores such as horseshoe vortices.

Ridgeline detection algorithms [16] and the higher order vortex identification method [19] require second spatial and total derivatives, respectively, which introduce significant uncertainties in the case of computational fluid dynamics (CFD) evaluations. The effect is further amplified for skewed and irregular numerical grids typical for swept and skewed turbomachines.

Unlike the ridge line and the higher order methods, the vorticity predictor – pressure corrector technique by Banks and Singer [20] does not rely on numerical derivatives, and the vortex skeleton is calculated based on local field variables only. The method uses predefined seed points to grow the vortex skeleton. Firstly, the following point in the vortex core is predicted with the vorticity vector. However, it is well-known that the vorticity vector may not align with the vortex core; thus, integrating along the vorticity vector does not follow the vortex skeleton. Therefore, in the corrector step, the pressure minimum corresponding to the vortex core is sought in the plane perpendicular to the vorticity vector at the predicted point. Likewise to the vorticity integral, a set of pressure minimum points do not automatically constitute a vortex core line as external flow features also affect the pressure distribution. However, the vortex skeleton is likely to be entirely identified with the combination of the predictor and corrector steps. These two steps are repeated to follow the vortex skeleton until the termination of the vortex line. The steps of the method are shown in Fig. 1.

Vinha et al. [21] successfully applied the Banks' approach for the unsteady Reynolds-averaged Navier-Stokes (URANS) simulation of a counter-rotating open rotor (CROR) engine TLV. The resulting vortex skeletons agreed with the λ_2 [12] and the Q criterion [13]. Also, it has been showed that the vorticity predictor – pressure corrector technique was capable of effectively identifying the TLV of a ducted low-speed fan [22, 23]. As highlighted by Vinha, the drawback of Banks' method is its sensitivity to seed positions.

The vortex core distance technique by Li and Carrica [24] defines the distance to the vortex core as the magnitude of the pressure gradient divided by half of the pressure Laplacian. For a more straightforward calculation, the Laplacian can be exchanged for the second invariant of the velocity gradient (Q). Isosurfaces of this variable are vortex tubes equidistant to the vortex core regardless of vortex size and strength. Finally, the Lagrangian average vorticity deviation (LAVD) method [25] might be utilized for vortex core localization. However, the model contains a high number of arbitrarily tunable parameters, and the recommendations for these are scarce [26].

Although the TLV wandering of axial flow turbomachines has been reported numerous times in both measurements and simulations, the characteristics of the wandering natural motion have not been quantified in a comprehensive manner. Thus, a technique for quantifying the TLV wandering of an axial fan based on unsteady Reynolds-averaged Navier-Stokes simulation and Banks' vorticity predictor – pressure corrector vortex core identification method [20] is presented in the current paper. The predictor-corrector method provides the instantaneous

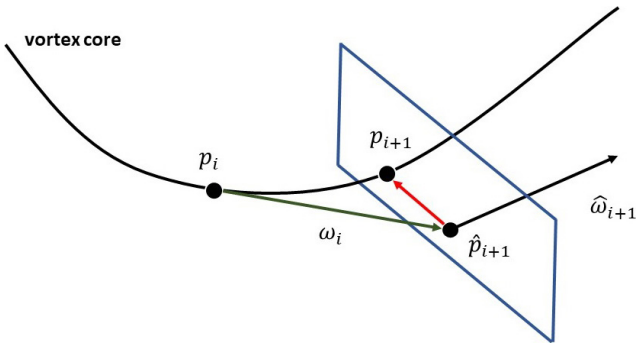

Fig. 1 Banks' vorticity predictor: pressure corrector vortex core line detection technique; p_i: initial seed position; ω_i: vorticity at the initial position; green arrow: predictor step; red arrow on blue plane: corrector step; p_{i+1}: final position

TLV trajectory; therefore, the extent of the TLV wandering motion can be determined by applying the process at different time instances. The presented technique, which has relatively low equipment or computational cost compared to measurements or other simulations, can be used to thoroughly investigate the TLV wandering phenomenon. The capabilities of the method are presented through a fan simulation case study.

2 Investigated axial flow fan

The investigated low-speed axial flow fan is a rotor-only configuration with five forward-skewed control vortex design blades. The blades had circular arch profiles with 1 mm thickness. The radii of the blade tips were r_b = 0.15 m with a 0.3 tip-to-hub ratio. The blade tip gap was set to 5% of the blade tip radius. The fan was investigated at 1400 RPM for the simulation. The corresponding mid-chord-based Reynolds number was 105000. For comparison, simulations were carried out also at 1120 and 1680 RPM (±20%). The fan was investigated in the design operating condition. The global flow coefficient (annulus area-averaged axial velocity normalized by the blade tip velocity) was $\Phi = 0.300$, and the total pressure rise coefficient (mass flow weighted average total pressure rise normalized by the dynamic pressure calculated with the blade tip velocity) was $\Psi_{tot} = 0.174$ at 1400 RPM.

3 Computational setup

CFD simulations were used to investigate the TLV wandering of the fan. The URANS numerical simulations were performed using the ANSYS Fluent 22R1 software [27]. The turbulence effects were modeled with Menter's k-ω shear stress transport (SST) turbulence model [28]. The air was assumed to be incompressible. The SIMPLE pressure-velocity coupling was used for the simulations. The time integration was executed with the second-order implicit scheme, while second-order upwinding was set for the numerical schemes.

Using the circumferential periodicity of the fan rotor, only a single blade passage was modeled with rotationally periodic boundaries. For the simulations, the frozen rotor approach was used with a prescribed rotating reference frame for the rotor zone, while the inlet and outlet ducts had a stationary reference frame. The simulation domain is shown in Fig. 2.

The simulations employed a 3 r_b long inlet duct section with velocity inlet. The specified velocity, turbulent kinetic energy, and specific turbulent dissipation rate

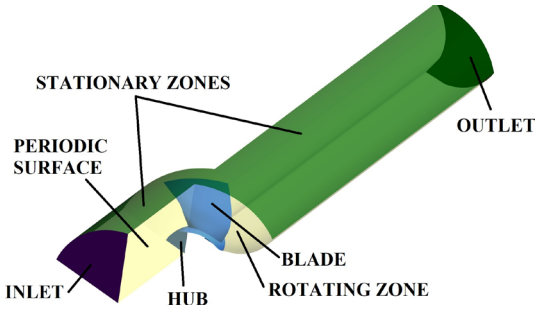

Fig. 2 Simulation domain

distributions were previously calculated using a fully developed periodic duct simulation. The free exhaust surface was set as a constant static pressure outlet at the end of the 10 rb long outlet duct; thus, the boundary conditions did not affect the fan operation.

In order to investigate the flow features near the blade tip, a well-refined numerical mesh was cleated for the tip region, while a coarser mesh was prescribed further away from the rotor tip to reduce computational costs. A structured O-grid mesh with 1 million hexahedral cells was prepared for the rotor. The blade was meshed with 75 and 60 cells in the streamwise and radial directions, respectively, with more refined mesh near the blade leading edge, trailing edge, and especially towards the blade tip. The domain was resolved with 120 cells circumferentially. The blade thickness was resolved with 20 cells, while the tip gap was divided with 25 cells radially. The H-grid duct meshes contained 150000 cells with high-resolution boundary layer meshes. Mesh sensitivity analysis was carried out through isotropic mesh adaptation. The resulting numerical mesh containing close to 9 million cells showed similar results to the used mesh with respect to the operating point (below 0.6% difference in total pressure rise) and efficiency (below 0.5% difference). At the same time, the vortex wandering location, amplitude, and frequency were identical for the two meshes. Thus, the used mesh was considered adequate. The surface mesh of the rotor blade can be seen in Fig. 3.

The unsteady simulations were initialized with 50 blade passes for the vortex wandering to develop. The complete development of the vortex wandering was verified by monitoring surface pressure tap fluctuation and the momentum oscillation acting on the rotor blade. After initialization, the flow field was sampled for ten blade passes. A single blade passing was resolved with 860 timesteps, and the data acquisition was initiated every 5 timesteps.

The vorticity predictor – pressure corrector vortex core line detection technique by Banks and Singer [20] was

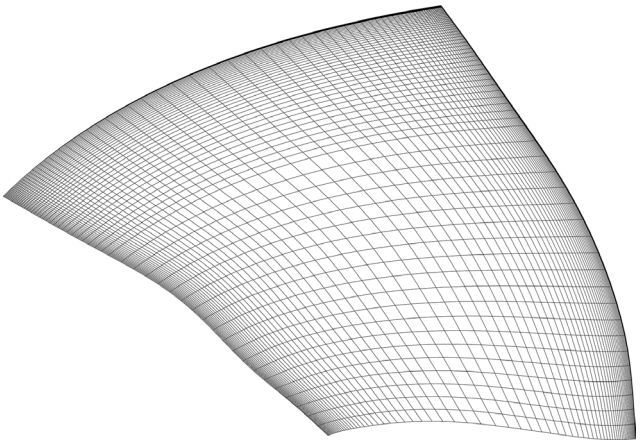

Fig. 3 The structured surface mesh of the rotor blade

found to be accurate, robust, and relatively independent of mesh quality; thus, it was found to be the most suitable for the application [22]. The used method is also favorable as it has relatively low computational costs compared to other ridge detection algorithms.

Banks' vorticity predictor – pressure corrector vortex core identification technique follows vortex skeletons from predefined seed points in two steps. The steps of the vortex line detection method are shown in Fig. 1. Starting from a seed point, the vortex detection algorithm in the first step predicts the vortex core direction based on the local vorticity vector. Following this, the prediction is corrected by searching for the pressure minimum on the plane perpendicular to the local vorticity at the predicted location. These two steps are repeated to follow the vortex skeleton.

The performance of the predictor-corrector method can be influenced by two input parameters. The initial step size determines the resolution of the vortex skeleton. It was found that 0.4% of the chord length step size proved adequate for the used mesh resolution.

The second parameter is the size of the corrector step surface perpendicular to the vorticity at the predicted intermediate point. The pressure minimum was sought for the evaluation on a square surface with 0.16% chord length edges. The ratio of step size and corrector surface edge length determines the maximum angular deviation between the vorticity and the vortex core line. With the given parameters, the maximum deviation was set as 15.9°.

As mentioned in Section 1, the drawback of Banks' method is its sensitivity to seed positions for the vortex skeleton to develop from. Near the blade tip leading edge, where the TLV originates, local separations and the solid wall surface disturb the pressure and vorticity fields, making seed localization at the blade tip impossible. For this reason, the seed was located at 10% chord length downstream of the blade leading edge using pressure minimum and vorticity maximum locations.

The simulation data were extracted at each cell center, and a hypersurface was interpolated for the whole investigated domain with the natural neighbor interpolation method. The effect of the numerical grid is somewhat visible in the detected vortex core lines as the structured mesh guides the ridge lines along the grid. Thus, a smoother resolution could have been attainable with a finer mesh. The vortex skeletons were terminated at the periodic interface surface of the rotating zone as the non-conforming mesh surfaces introduced significant uncertainties to the results. More details on the implementation of the vortex core identification method can be found in [22].

4 Results and discussion

Firstly, the developed flow field and vortical structures in the blade passage are investigated. Fig. 4 shows the vortex regions displayed by the Q criterion. The main TLV originates close downstream of the blade tip leading edge and rolls up while propagating downstream in the blade passage. A secondary tip leakage vortex also develops upstream of the blade tip trailing edge due to the relatively large tip gap size. Besides the tip leakage vortices, an induced vortex with an opposite rotational direction to the main TLV is visualized upstream of and parallel to the TLV. The developed vortical structures and flowfield match the results for low-speed axial flow fans reported in the literature [9, 29]. Fig. 4 shows a discontinuity in the iso-surfaces at the rotational periodic boundary caused by the non-conformal grid interface.

The predictor-corrector vortex core line identification technique could be applied to any simulation timestep. Since the aim of the present study was to determine the extent of the TLV wandering, only the main TLV and its unsteady behavior will be investigated in the forthcoming. Therefore, only the single most prominent seed corresponding to the TLV was chosen in the seeding process for all time steps. Fig. 5 shows the vortex core line calculated by the predictor-corrector method, the Q criterion iso-surface, and the vortex core distance technique by Li and Carrica [24] for a time instance. Based on Fig. 5, the predictor-corrector method is capable of determining the vortex core line of the TLV until the periodic boundary surface. Further analysis of the used technique was presented in [22].

Based on the vortex core detection technique applied for a single timestep, the TLV core is an asymmetric diverging

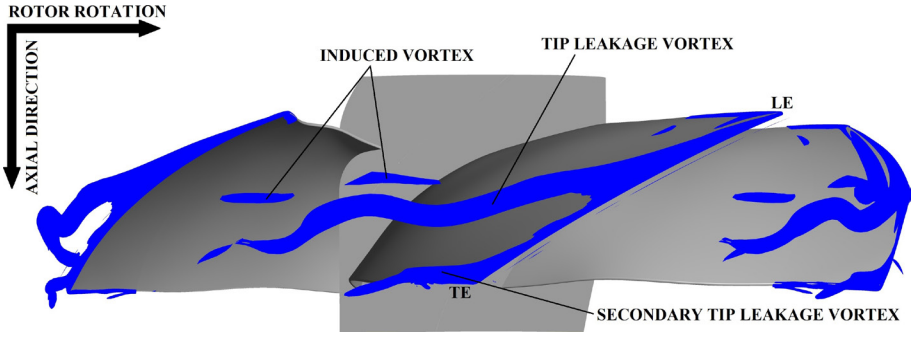

Fig. 4 The dominant vortical structure of the developed tip leakage flow highlighted by the Q criterion, Q = 2e6 1/s^2. LE: leading edge; TE: trailing edge

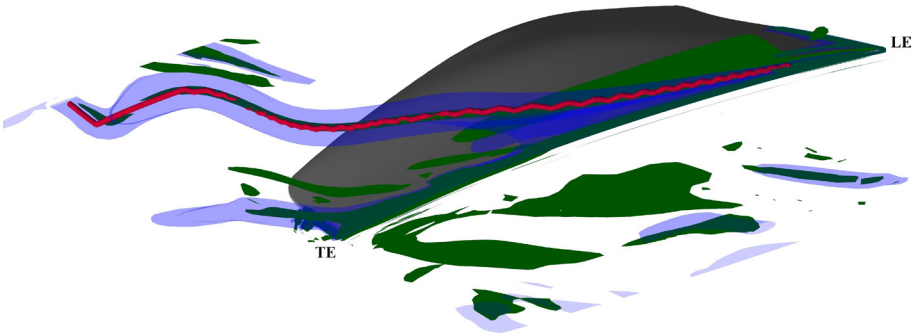

Fig. 5 The vortex core line calculated by the predictor-corrector method (red), the Q criterion iso-surfaces (blue, Q = 2e6 1/s^2), and the vortex core distance technique by Li and Carrica [24] (green). LE: leading edge; TE: trailing edge

spiral that follows the casing wall curvature as it propagates downstream in the blade passage. The spiraling vortex line had the largest displacement in the circumferential direction. These results agree well with the literature [2, 4, 5]. Also, it can be observed in Fig. 5 that the numerical mesh resolution had a significant influence on the detected vortex core trajectory. However, no filtering was applied to the calculated vortex core lines during post-processing to avoid unintentionally impairing the results.

Applying the vortex core detection method at multiple consecutive simulation timesteps illustrates the unsteady behavior of the TLV. The vortex wandering phenomenon of the TLV was investigated at planes perpendicular to the time-averaged vorticity for axial positions between 20% and 70% chord. The TLV core lines were linearly interpolated onto the investigated planes. Some of the investigated planes and the corresponding vortex core paths are depicted in Fig. 6. The vortex path for precisely five periods can be seen in Fig. 7 for the investigation planes corresponding to 50% and 70% chord axial positions. The extent of the vortex wandering was nondimensionalized with the tip chord length. The pattern reveals that the vortex moves around

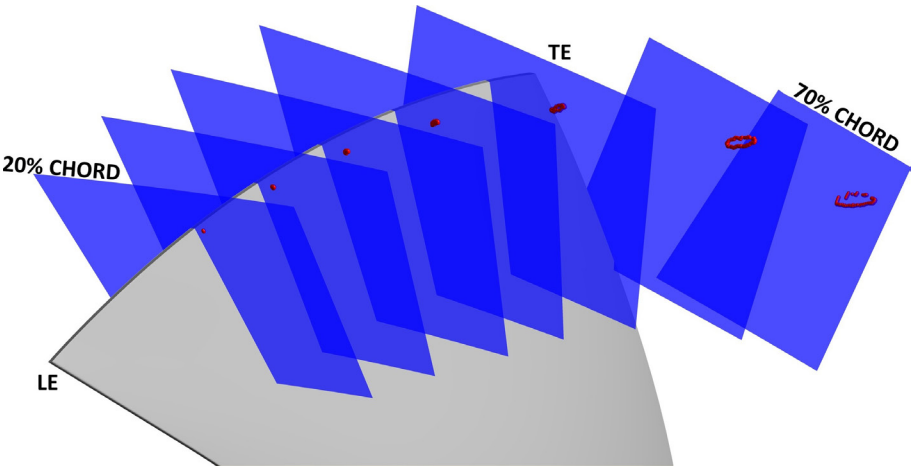

Fig. 6 Some of the investigated planes between 20% and 70% chord axial positions and the corresponding vortex core paths

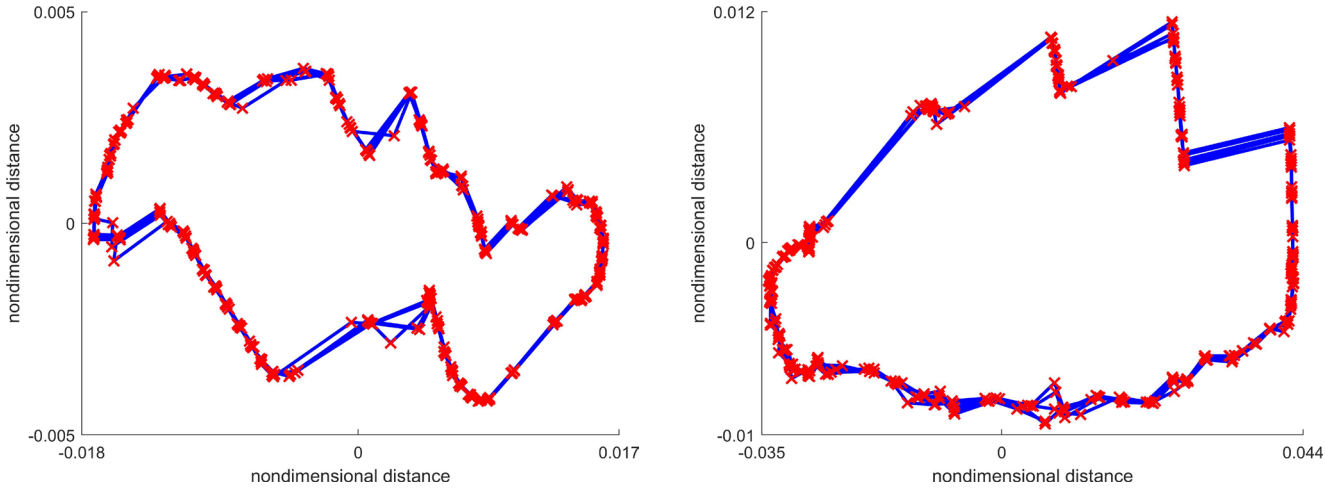

Fig. 7 Vortex core paths of five full periods on the investigated planes (a) at 50% chord axial position; (b) at 70% chord axial position

on an elliptical path periodically in the clockwise direction when seen from the upstream direction. Also, it can be observed in Fig. 7 that the numerical grid had a significant effect on the resolution of the detected vortex core paths.

Based on the vortex core paths in Fig. 7 it is clearly visible that the vortex wandering of the tip leakage vortex is entirely periodic, and the core trajectory repeats the same vortex core path. Contrarily, the PIV measurements concluded a more scattered, random-like vortex core placements [7, 8]. This can be explained by the undisturbed steady inflow conditions in the case of the URANS simulations. Also, the rotor geometry was assumed to be perfectly periodic without any manufacturing errors. Therefore, there were no disturbing influences for the simulations that would result in scattered, uneven core paths observed in the cases of PIV measurements. Also, the extent of the vortex wandering suggests that the instability of the vortex is flow-induced as the vortex wandering amplitude exceeds multiple grid cells. Therefore, it was concluded that the unsteadiness does not originate from numerical error or numerical instability.

The vortex wandering was also quantified for all investigated planes between 20–70% chord. The magnitude of the wandering motion was defined as the maximum distance between cores at the section planes. The largest displacements nondimensionalized with the tip chord length are depicted in Fig. 8 as a function of the axial position. Simulations with the same operating condition ($\Phi = 0.300$, $\Psi_{tot} = 0.174$) were carried out also at 1120 and 1680 RPM (±20% of the nominal 1400 RPM) for comparison. The nondimensionalized largest displacements of the vortex wandering in the investigated planes are also shown in Fig. 8 for the 1400 RPM rotation speed as a function of the axial position. The magnitude of the vortex wandering grew continuously along the path of the vortex core, apart from the small fluctuations caused by the mesh resolution. The wandering motion amplitude grows slowly up to 50% chord where it increases rapidly until the 70% chord limit by the periodic boundary surface. The different rotational speed simulations showed similar trends for the vortex wandering amplitude growth. Also, the order of magnitude of the wandering motion conforms with the literature as Jin et al. [7] reported tip leakage vortex core location displacement of 6.4% of the blade tip chord length at 50% chord length on a plane perpendicular to the chord line.

The frequency of the TLV wandering was also investigated. The frequency of the unsteady motion was calculated based on several full periods. The TLV wandering

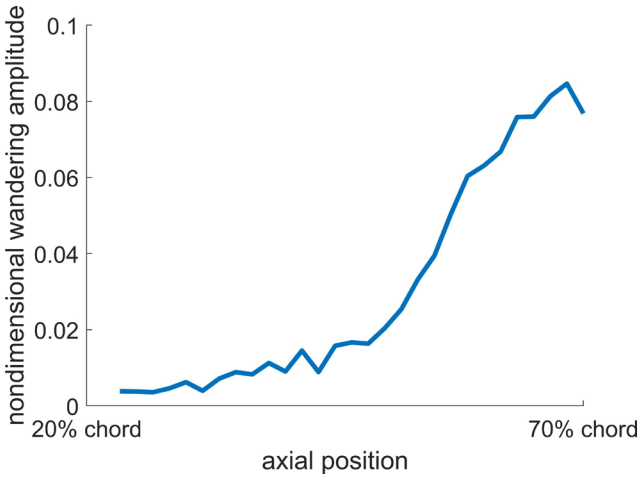

Fig. 8 The largest displacement of the TLV wandering as a function of axial position for the 1400 RPM rotational speed

frequency was 286 Hz in the case of the 1400 RPM simulation. The complementary simulations of 1120 and 1680 RPM had 225 and 339 Hz vortex wandering frequencies, respectively. The frequency of the vortex wandering is directly proportional to the rotational speed. Thus, these results agree well with the findings of Fukano and Jang [2].

The frequency of the vortex wandering can also be expressed with the nondimensional frequency called the Strouhal number. However, as discussed in Section 1, the method of nondimensionalizing the frequency is not straightforward. Applying the Strouhal number definition of Park et al. (blade tip radius and velocity) [10] and Boudet et al. (relative streamwise velocity at the blade tip and blade tip chord length) [9] for the results of the present study gives the Strouhal numbers St = 1.95 and 2.00, respectively, for the 1400 RPM case.

During the flow field data sampling for the vortex core detection, the forces acting on the blade surfaces were also monitored. Significant moment fluctuation was observed with a frequency identical to the vortex wandering frequency. The amplitude of the momentum fluctuation exceeded 3.7% of the time-averaged torque acting on the rotor. Thus, it was concluded that the moment fluctuation was produced by large pressure fluctuation created by the unsteady TLV motion. The pressure fluctuation is unfavorable as it may have multiple adverse effects. Surface pressure oscillation leads to potentially significant sound emission. Also, low-frequency momentum oscillation induces vibration, which causes premature wear and promotes structural failure.

5 Conclusion

In the present paper, a technique for investigating the tip leakage vortex wandering in a low-speed axial flow fan was introduced, and its capacities were demonstrated through a case study. The unsteady Reynolds-averaged Navier-Stokes simulations-based technique uses instantaneous vortex skeletons calculated with the vorticity predictor – pressure corrector vortex core line detection method by Banks and Singer [20]. The extent of the TLV wandering can be determined when applying the technique in consecutive time instances.

Using the technique, the TLV core line was identified as an asymmetric diverging spiral. The sequence of vortex core skeletons revealed that the vortex moves around on an elliptical path periodically in the clockwise direction when seen from the upstream direction. The spiraling vortex line had the largest displacement in the circumferential direction. Also, the magnitude of the vortex wandering amplitude grew slowly up to 50% chord, increasing rapidly until the 70% chord axial position.

The frequency of the TLV wandering was also assessed. Complementary simulations suggested that the frequency of the wandering motion was directly proportional to the rotational speed of the rotor. The blade tip radius and blade tip velocity based Strouhal number was 1.95. Moreover, significant moment fluctuation on the rotor blade caused by the wandering motion of the TLV was observed in the simulations.

Based on the above, the TLV wandering of an axial flow fan can be resolved with URANS simulations. Also, the URANS-based instantaneous vortex core line identification technique is suitable for investigating the natural unsteadiness of the TLV. This is supported by the results conforming to the scarce literature data.

Acknowledgement

Supported by the ÚNKP-23-3-II-BME-104 New National Excellence Program of the Ministry for Culture and Innovation from the source of the National Research, Development, and Innovation Fund. The research has been funded by the Hungarian National Research, Development, and Innovation Centre under contract No. K 143204. Project no. TKP-6-6/PALY-2021 has been implemented with the support provided by the Ministry of Culture and Innovation of Hungary from the National Research, Development and Innovation Fund, financed under the TKP2021-NVA funding scheme.

Nomenclature

Φ	Global flow coefficient
Ψ_{tot}	Total pressure rise coefficient
r_b	Blade tip radius
CROR	Counter-rotating open rotor
PIV	Particle image velocimetry
St	Strouhal number
TLV	Tip leakage vortex
URANS	Unsteady Reynolds-averaged Navier-Stokes simulation

References

[1] Longhouse R. E. "Control of tip-vortex noise of axial flow fans by rotating shrouds", Journal of Sound and Vibration, 58(2), pp. 201–214, 1978.
https://doi.org/10.1016/S0022-460X(78)80075-3

[2] Fukano, T., Jang, C.-M. "Tip clearance noise of axial flow fans operating at design and off-design condition", Journal of Sound and Vibration, 275(3–5), pp. 1027–1050, 2004.
https://doi.org/10.1016/S0022-460X(03)00815-0

[3] Benedek, T., Vad, J., Lendvai, B. "Combined acoustic and aerodynamic investigation of the effect of inlet geometry on tip leakage flow noise of free-inlet free-exhaust low-speed axial flow fans", Applied Acoustics, 187, 108488, 2022.
https://doi.org/10.1016/j.apacoust.2021.108488

[4] Tan, D., Li, Y., Wilkes, I., Miorini, R. L., Katz, J. "Visualization and Time-Resolved Particle Image Velocimetry Measurements of the Flow in the Tip Region of a Subsonic Compressor Rotor", ASME Journal of Turbomachinery, 137(4), 041007, 2015.
https://doi.org/10.1115/1.4028433

[5] Zhu, T., Lallier-Daniels, D., Sanjosé, M., Moreau, S., Carolus, T. "Rotating coherent flow structures as a source for narrowband tip clearance noise from axial fans", Journal of Sound and Vibration, 417, pp. 198–215, 2018.
https://doi.org/10.1016/j.jsv.2017.11.014

[6] Zeinali, M., Abbasi, S., Hajizadeh Aghdam, A. "Commencement and Development Processes of Flow Unsteadiness at Tip Clearance Region of a Low Speed Axial Compressor Rotor Blade Row", Periodica Polytechnica Mechanical Engineering, 61(4), pp. 288–295, 2017.
https://doi.org/10.3311/PPme.11113

[7] Jin, G.-Y., Ouyang, H., Wu, Y.-D., Du, Z.-H. "An experimental study of the unsteady characteristics of tip-leakage flow of axial fans with circumferential skewed blades at off-design conditions", Proceedings of the Institution of Mechanical Engineers, Part A: Journal of Power and Energy, 225(6), pp. 802–816, 2011.
https://doi.org/10.1177/0957650911404621

[8] Lee, H., Park, K., Choi, H. "Experimental investigation of tip-leakage flow in an axial flow fan at various flow rates", Journal of Mechanical Science and Technology, 33(3), pp. 1271–1278, 2019.
https://doi.org/10.1007/s12206-019-0227-z

[9] Boudet, J., Cahuzac, A., Kausche, P., Jacob, M. C. "Zonal Large-Eddy Simulation of a Fan Tip-Clearance Flow, With Evidence of Vortex Wandering", ASME Journal of Turbomachinery, 137(6), 061001, 2015.
https://doi.org/10.1115/1.4028668

[10] Park, K., Choi, H., Choi, S., Sa, Y., Kwon, O. "Unsteady Characteristics of Tip-Leakage Flow in an Axial Flow Fan", In: Proceeding of Tenth International Symposium on Turbulence and Shear Flow Phenomena, Chicago, IL, USA, 2017, pp. 623–627. ISBN 9780000000002
https://doi.org/10.1615/TSFP10.1060

[11] You, D., Wang, M., Moin, P., Mittal, R. "Vortex Dynamics and Low-Pressure Fluctuations in the Tip-Clearance Flow", ASME Journal of Fluids Engineering, 129(8), pp. 1002–1014, 2007.
https://doi.org/10.1115/1.2746911

[12] Jeong, J., Hussain, F. "On the identification of a vortex", Journal of Fluid Mechanics, 285, pp. 69–94, 1995.
https://doi.org/10.1017/S0022112095000462

[13] Hunt, J. C. R., Wray, A. A., Moin, P. "Eddies, Streams, and Convergence Zones in Turbulent Flows", Studying Turbulence Using Numerical Simulation Databases, 2, pp. 193–208, 1988.

[14] Epps, B. P. "Review of Vortex Identification Methods", presented at 55th AIAA Aerospace Sciences Meeting, Grapevine, TX, USA, Jan. 09–13., 2017.
https://doi.org/10.2514/6.2017-0989

[15] Levy, Y., Degani, D., Seginer, A. "Graphical Visualization of Vortical Flows by Means of Helicity", AIAA Journal, 28(8), pp. 1347–1352, 1990.
https://doi.org/10.2514/3.25224

[16] Miura, H., Kida, S. "Identification of Tubular Vortices in Turbulence", Journal of the Physical Society of Japan, 66(5), pp. 1331–1334, 1997.
https://doi.org/10.1143/jpsj.66.1331

[17] Jiang, M., Machiraju, R., Thompson, D. "A Novel Approach To Vortex Core Region Detection", In: VisSym02: Joint Eurographics - IEEE TCVG Symposium on Visualization, Barcelona Spain, 2002, pp. 217–225. ISBN 978-1-58113-536-7
https://doi.org/10.2312/VisSym/VisSym02/217-225

[18] Sujudi, D., Haimes, R. "Identification of Swirling Flow in 3D Vector Fields", presented at 12th Computational Fluid Dynamics Conference, San Diego, CA, USA, Jun. 19–22., 1995.
https://doi.org/10.2514/6.1995-1715

[19] Roth, M., Peikert, R. "A higher-order method for finding vortex core lines", In: Proceedings Visualization '98 (Cat. No.98CB36276), 1998, pp. 143–150. ISBN 0-8186-9176-X
https://doi.org/10.1109/VISUAL.1998.745296

[20] Banks, D. C., Singer, B. A. "A predictor-corrector technique for visualizing unsteady flow", IEEE Transactions on Visualization and Computer Graphics, 1(2), pp. 151–163, 1995.
https://doi.org/10.1109/2945.468404

[21] Vinha, N., Vallespin, D., Valero, E., de Pablo, V., Cuesta-Lopez, S. "Numerical prediction of vortex trajectories and vortex–blade interaction on the CROR engine", Aircraft Engineering and Aerospace Technology, 92(9), pp. 1345–1356, 2020.
https://doi.org/10.1108/AEAT-03-2020-0044

[22] Lendvai, B., Benedek, T. "Application of a Vortex Identification Method for Quantifying the Tip Leakage Vortex Wandering in a Low-Speed Axial Fan Case Study", presented at 15th European Conference on Turbomachinery Fluid dynamics & Thermodynamics, Budapest, Hungary, Apr. 24–28., 2023.
https://doi.org/10.29008/ETC2023-231

[23] Balla, E., Kovács, K. A., Lendvai, B. "Comparison of Vortex Detection Methods on the Numerical Simulation of Tip Leakage Flow of a Low-Speed Axial Fan", In: Proceedings of the ASME Turbo Expo 2024: Turbomachinery Technical Conference and Exposition, London, UK, 2024, V006T10A002. ISBN 978-0-7918-8798-1
https://doi.org/10.1115/GT2024-121322

[24] Li, J., Carrica, P. M. "A Simple Approach for Vortex Core Visualization", ASME Journal of Fluids Engineering, 142(5), 051504, 2020.
https://doi.org/10.1115/1.4045999

[25] Haller, G., Hadjighasem, A., Farazmand, M., Huhn, F. "Defining coherent vortices objectively from the vorticity", Journal of Fluid Mechanics, 795, pp. 136–173, 2016.
https://doi.org/10.1017/jfm.2016.151

[26] Kovács, K. A., Balla, E. "Parameter Identification of the Lagrangian-averaged Vorticity Deviation Vortex Detection Method Through the Investigation of Fluid Flow Around Solid Bodies", Periodica Polytechnica Mechanical Engineering, 67(4), pp. 293–302, 2023.
https://doi.org/10.3311/PPme.22874

[27] ANSYS "ANSYS Fluent, (22R1)", [computer program] Available at: https://www.ansys.com/products/fluids/ansys-fluent [Accessed: 05 August 2022]

[28] Menter, F. R. "Zonal Two Equation k-ω Turbulence Models for Aerodynamic Flows", presented at 23rd Fluid Dynamics, Plasmadynamics, and Laser Conference, Orlando, FL, USA, Jul. 06–09., 1993.
https://doi.org/10.2514/6.1993-2906

[29] Decaix, J., Balarac, G., Dreyer, M., Farhat, M., Münch, C. "RANS and LES computations of the tip-leakage vortex for different gap widths", Journal of Turbulence, 16(4), pp. 309–341, 2015.
https://doi.org/10.1080/14685248.2014.984068